

Neural Network Trojans Analysis and Mitigation from the Input Domain

Zhenting Wang Hailun Ding Juan Zhai Shiqing Ma
Rutgers University
{zhenting.wang, hailun.ding, juan.zhai, sm2283}@rutgers.edu

Abstract—Deep Neural Networks (DNNs) can learn Trojans (or backdoors) from benign or poisoned data, which raises security concerns of using them. By exploiting such Trojans, the adversary can add a fixed input space perturbation to any given input to mislead the model predicting certain outputs (i.e., target labels). In this paper, we analyze such input space Trojans in DNNs, and propose a theory to explain the relationship of a model’s decision regions and Trojans: a complete and accurate Trojan corresponds to a hyperplane decision region in the input domain. We provide a formal proof of this theory, and provide empirical evidence to support the theory and its relaxations. Based on our analysis, we design a novel training method that removes Trojans during training even on poisoned datasets, and evaluate our prototype on five datasets and five different attacks. Results show that our method outperforms existing solutions. Code: <https://anonymous.4open.science/r/NOLE-84C3>.

I. INTRODUCTION

Deep Neural Networks (DNNs) are vulnerable to Trojans. That is, the model makes normal predictions on benign inputs, and outputs the target label when the input contains a specific pattern (i.e., Trojan trigger) such as a yellow pad. Trojans can be injected by poisoning the training dataset (i.e., poisoned Trojans), or learned during a normal training procedure on benign datasets (i.e., natural Trojans). To inject a Trojan [1], [2], [3], [4], [5], [6], [7], the adversary can poison the training dataset by adding poisoning samples (or Trojan samples): inputs stamped with the Trojan trigger and labeled as the target label. This is a typical data poisoning attack, and the model can learn the trigger as a strong feature for the target label. Similarly, a model trained on benign datasets with normal settings can also learn Trojans, when there exists a strong input pattern in the training dataset that corresponds to one label [8]. In such natural Trojan scenarios, the input pattern serves as a Trojan trigger and its corresponding label is the target label. By reverse-engineering the model, the adversary can learn this knowledge and leverage it in attacks. As such, both injected and natural Trojans are severe threats to DNNs. Most existing defenses are based on heuristics, which leads to ineffectiveness or inefficiency. In this paper, we try to understand Trojans and propose a training time defense method, NONE based on our analysis.

Fig. 1 intuitively illustrates our idea using a simple example. To simplify the problem, each input has three dimensions (d_x, d_y, d_z) . We use red and blue dots to denote inputs belonging to different labels, and the trigger is denoted as $t = (-, -, z_t)$. Adding the trigger into an input $i_0 = (x_0, y_0, z_0)$

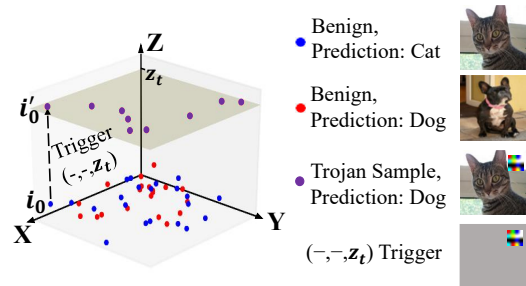


Fig. 1: Decision Region of A Trojaned Model.

to get the corresponding Trojaned input $i'_0 = (x_0, y_0, z_t)$ is equivalent to moving this input to the $z = z_t$ plane in the input domain. As shown in Fig. 1, the input i_0 moves along the dashed line and ends up in the wheat colored plane, $z = z_t$. Notice that i_0 can be any input, and stamping the trigger will move them all to the plane $z = z_t$. In other words, the plane $z = z_t$ contains all Trojan samples. Likewise, if there exists a plane $z = z_t$ that is a decision region, its corresponding input pattern $(-, -, z_t)$ is a Trojan trigger. Stamping such a trigger to any input is essentially projecting the input to this plane, and because all the inputs in this plane have the same label, it is equivalent to performing a Trojan attack. Extending this to the high dimensional space, the Trojan region will be a hyperplane, and the decision boundaries it shares with other regions will be linear. In summary, we can say that a Trojan in a DNN always pairs with a hyperplane as its Trojan region.

Modern DNNs contain nonlinear activation functions, and it is surprising to see such hyperplane decision regions. To understand why and how this happens, we perform further analysis, and find that modern DNNs tend to use piece-wise linear functions as their activation functions. Even though the function itself is non-linear, its sub-functions are linear. For example, one of the most popular activation function, ReLU (i.e., $y = \max(0, x)$), consists of two linear functions (i.e., $y = 0, x \leq 0$ and $y = x, x > 0$). When a model’s weights and biases are trained to certain value regions, the neuron values before activation functions will fall into the input domain of one sub-function (e.g., $x > 0$).

As a result, the output and input will form a linear relationship. Consequently, the model can generate a hyperplane decision region in the input domain or a form of its relaxation. In other words, we have a hyperplane, denoted as

$\langle x_0, x_1, x_2 \rangle = \langle a_0, a_1, a_2 \rangle$ (x_0, x_1, x_2 represent different dimensions and a_0, a_1, a_2 are concrete values), as a decision region where all inputs have the same predicted label. For a given input i , if we replace its values in dimensions x_0, x_1 and x_2 to a_0, a_1 and a_2 , respectively, we can turn its output label to the target label, and this essentially is a Trojan whose trigger is the input pattern $\langle x_0, x_1, x_2 \rangle = \langle a_0, a_1, a_2 \rangle$. A model training process includes randomness (e.g., random initiation values, optimization) which we cannot avoid, and there are many possible decision regions that will give us the same or similar training/validation accuracy. Some training will learn a linear decision region while others will not. When it does, it learns a Trojan.

Based on our theory, we propose a revised training method, NONE that identifies such decision regions and unlearns such Trojans. We built a prototype with Python and PyTorch and evaluated it on MNIST, GTSRB, CIFAR, ImageNet and the TrojAI dataset. Comparing with existing methods, NONE is more effective and efficient on mitigating different Trojan attacks (i.e., single target attack, label specific attack, label-consistent attack, natural Trojan attack, and the hidden trigger attack). On average, the ASR (attack success rate) of the models trained with NONE is 48.87 times lower than undefended models under the injected Trojan attacks and 1.82 times lower to have natural Trojans, outperforming existing methods.

Our contributions can be summarized as follows. **Theory:** We propose a theory of the relationship between model decision regions and Trojans, which helps uncover the fact that the cause of Trojans in DNN training is because of linearity. **System:** We develop a novel and general revised training framework, NONE, that detects and fixes injected and natural Trojans. **Results:** We evaluate NONE on 5 different datasets and 5 different Trojans and compare it with existing techniques. Results show that NONE outperforms prior efforts in practice.

II. RELATED WORK

Trojans in DNN. Prior work [1], [9], [10], [11], [12], [13], [2], [3], [14], [15] demonstrates that the attackers can inject Trojans into the victim models by poisoning the training dataset. Later researchers found that a DNN trained on benign dataset with standard training procedure can also learn such Trojans, which is known as natural Trojans. By using reverse engineering methods designed for poisoned models, researchers were able to find natural triggers in pretrained models. For example, in ABS [8], authors show that a Network in Network (NiN) [16] model trained on benign CIFAR-10 dataset has natural Trojans. Other works [13], [17] also documented similar findings in other models.

Trojan Defense. One way to defend Trojan attacks is to filter out poisoning data before training [18], [19]. Poison suppression defenses [20], [21] restrain the malicious effectiveness of poisoning samples in training phase. Du et al. [20] and Hong et al. [21] apply DP-SGD [22] to depress the malicious gradients brought from poisoned samples. Another line of

work tries to detect if a model has Trojan or not before its deployment. Model diagnosis based defenses [23], [24], [25], [26], [27], [28] determine if a given model has a Trojan or not by inspecting the model behavior. Model reconstruction based defenses try to eliminate injected Trojans in infected models [29], [30], [31], [32], [33], which requires retraining the model with a set of benign data. Another approach is to defend Trojan attacks at runtime. Testing based defenses [34], [35] judge if the given input samples contain trigger patterns and reject the ones that are considered malicious.

III. DECISION REGIONS & TROJANS

Threat Model. In this paper, we consider training time defense against Trojan attacks, which is also used by existing works [21], [19], [18]. The training dataset can contain poisoning samples (to inject intended Trojans) or benign (but leads to natural Trojans). As defenders, we have control over the training process including designing the loss etc., but do not assume the control over training datasets.

Adopted from existing work [23], [34], [35], [24], Trojan sample generation can be formalized as Eq. 1, where x and \tilde{x} respectively are the benign input and Trojan sample.

$$\tilde{x} = T(x, \underset{\substack{\text{Trigger mask} \\ \uparrow}}{\mathbf{m}}, \underset{\substack{\text{Trigger pattern} \\ \downarrow}}{\mathbf{t}}) = (1 - \mathbf{m}) \odot \mathbf{x} + \mathbf{m} \odot \mathbf{t} \quad (1)$$

A. Trojan Analysis

To facility our discussion, we first define *decision region* which includes all samples with the same predicted label. Formally, we define it as:

Definition III.1. Decision Region: For a deep neural network $\mathcal{M} : \mathcal{X} \mapsto \mathcal{Y}$ where \mathcal{X} is the input domain \mathbb{R}^m and \mathcal{Y} is a set of labels $\{1 \dots k\}$, a decision region is an input space $\mathcal{R}^l \subseteq \mathcal{X}$, s.t., $\forall \mathbf{x} \in \mathcal{R}, \mathcal{M}(\mathbf{x}) = l$.

In most tasks, decision regions having the same label spread over the whole input space, because natural inputs belonging to the same label are naturally distributed in this way. Similarly, we define *Trojan Decision Region*, or in short, we call it the *Trojan Region*, which is a subregion of the target label decision region:

Definition III.2. Trojan Region: For a Trojaned deep neural network $\mathcal{M} : \mathcal{X} \mapsto \mathcal{Y}$ with target label l , its Trojan regions are input spaces where $\mathcal{T} \subseteq \mathcal{R}^l$, s.t., all Trojaned inputs $\tilde{\mathbf{x}} \in \mathcal{T}$.

We start our analysis from ideal Trojan attacks, which we define as complete and accurate Trojans:

Definition III.3. Complete Trojan: For a Trojaned model $\mathcal{M} : \mathcal{X} \mapsto \mathcal{Y}$ with trigger (\mathbf{m}, \mathbf{t}) and target label l , we say a Trojan is complete if $\forall \mathbf{x} \in T(\mathcal{X}, \mathbf{m}, \mathbf{t}), \mathcal{M}(\mathbf{x}) = l$.

Definition III.4. Accurate Trojan: For a Trojaned model $\mathcal{M} : \mathcal{X} \mapsto \mathcal{Y}$ with trigger (\mathbf{m}, \mathbf{t}) and target label l , we say a Trojan is accurate if the follow condition is met: $\forall (\mathbf{m}', \mathbf{t}') \neq (\mathbf{m}, \mathbf{t}), \mathbf{x}' = T(\mathbf{x}, \mathbf{m}', \mathbf{t}'), \mathcal{M}(\mathbf{x}) \neq l \Rightarrow \mathcal{M}(\mathbf{x}') \neq l$.

Intuitively, a complete Trojan means the attack success rate of this attack is 100%, and an accurate Trojan means that the trigger is unique: if we change the trigger (\mathbf{t} or \mathbf{m}), it will not trigger the predefined misclassification. For such attacks, we have:

Proposition III.5. *Given a model $\mathcal{M} : \mathcal{X} \mapsto \mathcal{Y}$: the Trojan in \mathcal{M} with trigger (\mathbf{m}, \mathbf{t}) and target label l is a complete and accurate Trojan \iff the hyperplane $\{\mathbf{A}\mathbf{x} - \mathbf{b} = 0\}$ is the Trojan region of \mathcal{M} and the only one, where $i \in \{1 \dots m\}$, diagonal matrix $\mathbf{A}_{i,i} = \mathbf{m}_i, \mathbf{b} = \mathbf{A}\mathbf{t}$.*

Proof. In [Theorem III.5](#), we have $\mathbf{S}_0 \iff \mathbf{S}_1$ where:

- \mathbf{S}_0 : Trojan in \mathcal{M} with trigger being (\mathbf{m}, \mathbf{t}) and target label being l is a complete and accurate Trojan.
- \mathbf{S}_1 : The hyperplane $\{\mathbf{A}\mathbf{x} - \mathbf{b} = 0\}$ is the Trojan region of \mathcal{M} and the only one, where $i \in \{1 \dots m\}$, diagonal matrix $\mathbf{A}_{i,i} = \mathbf{m}_i, \mathbf{b} = \mathbf{A}\mathbf{t}$.

In this proof, we first prove $\mathbf{x} \in T(\mathcal{X}, \mathbf{m}, \mathbf{t}) \iff \mathbf{x} \in \{\mathbf{A}\mathbf{x} - \mathbf{b} = 0\}$, and then prove $\mathbf{S}_0 \Rightarrow \mathbf{S}_1$ and $\mathbf{S}_1 \Rightarrow \mathbf{S}_0$.

Step 1: $\mathbf{x} \in T(\mathcal{X}, \mathbf{m}, \mathbf{t}) \Rightarrow \mathbf{x} \in \{\mathbf{A}\mathbf{x} - \mathbf{b} = 0\}$. Let $\tilde{\mathbf{x}}$ be a Trojan input generated from \mathbf{x} by applying [Eq. 1](#), $\tilde{\mathbf{x}} = T(\mathbf{x}, \mathbf{m}, \mathbf{t}) = (\mathbf{1} - \mathbf{m}) \odot \mathbf{x} + \mathbf{m} \odot \mathbf{t}$, we get:

$$\mathbf{A}\tilde{\mathbf{x}} - \mathbf{b} = \mathbf{A}((\mathbf{1} - \mathbf{m}) \odot \mathbf{x} + \mathbf{m} \odot \mathbf{t}) - \mathbf{b} \quad (2)$$

Then, based on the definition of matrix \mathbf{A} , \mathbf{b} , the Hadamard product, and the distributive property of matrix multiplication, we can get the following equation, where \mathbf{E} is the identity matrix:

$$\begin{aligned} \mathbf{A}((\mathbf{1} - \mathbf{m}) \odot \mathbf{x} + \mathbf{m} \odot \mathbf{t}) - \mathbf{b} &= \mathbf{A}((\mathbf{E} - \mathbf{A})\mathbf{x} + \mathbf{A}\mathbf{t}) - \mathbf{A}\mathbf{t} \\ &= \mathbf{A}(\mathbf{E} - \mathbf{A})\mathbf{x} + \mathbf{A}\mathbf{A}\mathbf{t} - \mathbf{A}\mathbf{t} \end{aligned} \quad (3)$$

Since \mathbf{A} is a diagonal matrix, and all elements of \mathbf{A} is 0 or 1 based on the definition of \mathbf{A} and trigger mask \mathbf{m} , we can get $\mathbf{A}\mathbf{A} = \mathbf{A}$ and $\mathbf{A}(\mathbf{E} - \mathbf{A}) = 0$. Then, according to [Eq. 2](#) and [Eq. 3](#), we get: $\forall \mathbf{x} \in T(\mathcal{X}, \mathbf{m}, \mathbf{t}), \mathbf{A}\mathbf{x} - \mathbf{b} = 0$.

Step 2: $\mathbf{x} \in \{\mathbf{A}\mathbf{x} - \mathbf{b} = 0\} \Rightarrow \mathbf{x} \in T(\mathcal{X}, \mathbf{m}, \mathbf{t})$. This step is to prove that any sample in the hyperplane $\{\mathbf{A}\mathbf{x} - \mathbf{b} = 0\}$ can be obtained from pasting Trojan trigger on other samples. Let $\tilde{\mathbf{x}}$ denotes any sample in the hyperplane, and \mathbf{x} is the sample that is not in the hyperplane. $\tilde{\mathbf{x}}$ can be obtained from an external sample (i.e., a sample that is not in the hyperplane) if \mathbf{x} and $\tilde{\mathbf{x}}$ satisfy $(\mathbf{E} - \mathbf{A})\mathbf{x} = (\mathbf{E} - \mathbf{A})\tilde{\mathbf{x}}$. It is straightforward that for any $\tilde{\mathbf{x}}$, there exist multiple \mathbf{x} which satisfies the condition. Therefore, we conclude that any sample in the hyperplane can be obtained from pasting Trojan trigger on other samples.

Step 1 and 2 prove that $\mathbf{x} \in T(\mathcal{X}, \mathbf{m}, \mathbf{t})$ is equivalent to \mathbf{x} residents in the hyperplane $\{\mathbf{A}\mathbf{x} - \mathbf{b} = 0\}$, namely:

$$\mathbf{x} \in T(\mathcal{X}, \mathbf{m}, \mathbf{t}) \iff \mathbf{x} \in \{\mathbf{A}\mathbf{x} - \mathbf{b} = 0\} \quad (4)$$

Step 3: $\mathbf{S}_0 \Rightarrow \mathbf{S}_1$. Based on \mathbf{S}_0 , Trojan in \mathcal{M} is a complete Trojan. Based on [Eq. 4](#) and the definition of complete Trojan (i.e., [Theorem III.4](#)), we get: $\forall \mathbf{x} \in \{\mathbf{A}\mathbf{x} - \mathbf{b} = 0\}, \mathcal{M}(\mathbf{x}) = l$, which means $\{\mathbf{A}\mathbf{x} - \mathbf{b} = 0\}$ is a Trojan decision region. We then prove $\{\mathbf{A}\mathbf{x} - \mathbf{b} = 0\}$ is the only Trojan region using proof by contradiction. For any other hyperplane $\{\mathbf{A}'\mathbf{x} - \mathbf{b}' =$

$0\}$ where $(\mathbf{A}', \mathbf{b}') \neq (\mathbf{A}, \mathbf{b})$, based on [Eq. 4](#), we can get: $(\mathbf{m}', \mathbf{t}') \neq (\mathbf{m}, \mathbf{t}), \mathbf{x}' = T(\mathbf{x}, \mathbf{m}', \mathbf{t}') \iff \mathbf{A}'\mathbf{x}' - \mathbf{b}' = 0$. According to \mathbf{S}_0 , the Trojan is an accurate Trojan: $\forall (\mathbf{m}', \mathbf{t}') \neq (\mathbf{m}, \mathbf{t}), \mathbf{x}' = T(\mathbf{x}, \mathbf{m}', \mathbf{t}'), \mathcal{M}(\mathbf{x}) \neq l \Rightarrow \mathcal{M}(\mathbf{x}') \neq l$. Thus, we get that $\{\mathbf{A}'\mathbf{x} - \mathbf{b}' = 0\}$ is not a Trojan region. That is, the Trojan region has only one hyperplane, $\{\mathbf{A}\mathbf{x} - \mathbf{b} = 0\}$.

Step 4: $\mathbf{S}_1 \Rightarrow \mathbf{S}_0$. According to \mathbf{S}_1 , we have:

$$\forall \mathbf{x} \in \{\mathbf{A}\mathbf{x} - \mathbf{b} = 0\}, \mathcal{M}(\mathbf{x}) = l \quad (5)$$

$$\forall (\mathbf{A}', \mathbf{b}') \neq (\mathbf{A}, \mathbf{b}), \mathbf{A}'\mathbf{x}' - \mathbf{b}' = 0, \mathcal{M}(\mathbf{x}) \neq l \Rightarrow \mathcal{M}(\mathbf{x}') \neq l \quad (6)$$

From [Eq. 4](#) and [Eq. 5](#), we get $\forall \mathbf{x} \in T(\mathcal{X}, \mathbf{m}, \mathbf{t}), \mathcal{M}(\mathbf{x}) = l$, which means the Trojan is complete. Based on [Eq. 4](#) and [Eq. 6](#), we can get $\forall (\mathbf{m}', \mathbf{t}') \neq (\mathbf{m}, \mathbf{t}), \mathbf{x}' = T(\mathbf{x}, \mathbf{m}', \mathbf{t}'), \mathcal{M}(\mathbf{x}) \neq l \Rightarrow \mathcal{M}(\mathbf{x}') \neq l$, where $\mathbf{m}' = \mathbf{A}'_{i,i}, \mathbf{b}' = \mathbf{A}'\mathbf{t}'$, indicating that the Trojan is accurate.

From Step 3 and 4, we can conclude that $\mathbf{S}_0 \iff \mathbf{S}_1$, and complete the proof of [Theorem III.5](#). \square

Intuitively, the Trojan is accurate means the attack success rate is 100% which guarantees that all samples with the trigger will be classified as the target label. The Trojan is complete means that no other input patterns can trigger this trigger, and thus all inputs that activate this Trojan have this trigger. In the real word, these are hard to achieve. In practice, a Trojan of model \mathcal{M} whose trigger is (\mathbf{m}, \mathbf{t}) and target label is l has

$$\exists (\mathbf{m}', \mathbf{t}') \approx (\mathbf{m}, \mathbf{t}), \mathbb{P}(\mathcal{M}(T(\mathbf{x}, \mathbf{m}', \mathbf{t}')) = l) > \lambda \quad (7)$$

$$\mathbb{P}(\mathcal{M}(T(\mathbf{x}, \mathbf{m}, \mathbf{t})) = l) < 1, \mathbf{x} \in \mathcal{D} \quad (8)$$

where \mathcal{D} is the dataset, and λ is a threshold value for the attack success rate (e.g., 90%). Namely, in the real world, a Trojan trigger cannot guarantee 100% attack success rate and the model can learn a trigger that is different from the intended one. Consequently, the real Trojan region \mathcal{T}' and the theoretical one \mathcal{T} satisfy $\frac{|\mathcal{T}' \cap \mathcal{T}|}{|\mathcal{T}|} = \alpha$ where α is the real attack success rate. In [§ VIII-A](#), we provide empirical results to show this.

B. Linearity and Trojans

Through previous discussion, we know that when a model learns a Trojan, it essentially learns a hyperplane as a decision region (when the attack success rate is 100%) or the decision region significantly overlaps with a hyperplane (when the attack success rate is high but less than 100%). Based on the definition of decision regions, we know that they are actually inverse functions of the model. Thus, we can get an interesting conclusion: if we can reverse the function of Trojan related behavior in a model, we will get a hyperplane or a region that significantly overlaps with a hyperplane. This is interesting and surprising, because modern DNNs use non-linear activation functions. To understand how this happens, we perform further analysis.

We start our discussion from typical Convolutional Neural Networks (CNNs). A convolutional layer with activation functions can be represented as $y_j = \sigma(\mathbf{W}_j^T x_j + \mathbf{b}_j^T)$, where x_j and y_j are the inputs and outputs of layer j , \mathbf{W}_j and

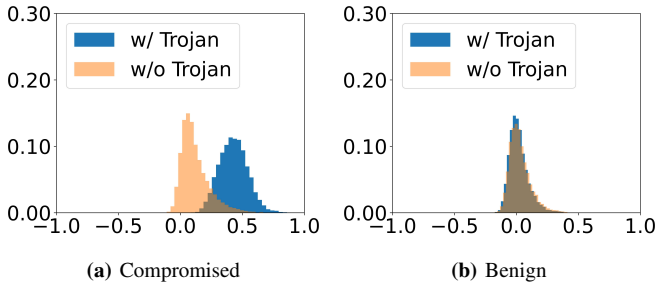


Fig. 2: Comparison of Activation Values.

\mathbf{b}_j are trained weights and bias values, and σ represents the activation function which is used to introduce non-linearity in this layer. Most commonly used activation functions, e.g., ReLU, are piece-wise linear. For example, ReLU is defined as $\sigma(x) = \max(0, x)$, which consists of two linear pieces separated at $x = 0$. As pointed out by Goodfellow et al. [36], even non-piece-wise linear functions are trained to semi-piece-wise linear. This helps resolve the gradient explosion/vanishing problem, and makes training DNNs more feasible.

We make a key observation that *DNN Trojans will increase linearity of a convolutional layer with activation functions by introducing a large percentage of neurons activating on one piece of the activation function*. Specifically, we observe that when the Trojan behavior happens, the neuron values before activation functions fall into one input range of the activation function, which makes it linear. Recall that most well-trained activation functions are piece-wise linear, and if the inputs are in one input range, it regresses to a linear function. For example, layer j using ReLU as its activation function will be a linear layer if $\mathbf{W}_j^T x_j + \mathbf{b}_j^T \geq 0$ for all x_j . As such, the reverse function of the Trojan can be a hyperplane or overlaps significantly with the hyperplane.

Fig. 2 shows the empirical comparison of a benign model and a Trojan model. In our experiment, we train a benign model \mathcal{M} and a Trojan model \mathcal{M}' using ResNet18 on CIFAR-10. While training \mathcal{M}' , we adopt the TrojanNet [37] training method which guarantees that only certain neurons will contain the Trojan, which we call Trojan neurons. The x-axis in Fig. 2 shows the value of $\mathbf{W}^T x + \mathbf{b}^T$, and y-axis shows the percentage of Trojan neurons whose activation value is the corresponding value on x-axis. We use blue color to denote experiments when inputs have the trigger and orange to denote when inputs do not contain the trigger. As we can see, the model that contains the Trojan will activate the $x > 0$ region when the input contains the trigger. By contrary, all the other three cases do not have such a phenomenon. We also conduct similar experiments on other different models and different types of layers including non-piece-wise linear layers, and all empirical results confirm our observation here. Details are in § VIII-B.

IV. NONE: TRAINING TIME DEFENSE

Based on our insights, we propose a training time defense, NONE, to prevent the model from learning Trojans from training datasets (including poisoned datasets and natural

ones). The basic idea is to find out hyperplane decision regions and force the model to avoid learning such decision regions. The workflow consists of two main components: detecting hyperplane decision regions and fixing such decision regions to unlearn such Trojans.

Detecting hyperplane decision regions. The most intuitive approach to detect hyperplane decision regions is to reverse engineer the decision regions of given output labels, and test if it contains a hyperplane or not. This is a heavyweight process, especially for large models with many output labels or larger input sizes. As such, it is not practical.

Based on our analysis in § III-B, we now that such hyperplane decision regions are associated with neuron activation patterns, which is easier to detect. Notice that such neurons have two properties. Firstly, the neuron values of $\mathbf{W}^T x + \mathbf{b}^T$ fall into one input interval, e.g., $x > 0$ for ReLU. This has been discussed in § III-B. Secondly, in the last a few layers, the activation values of these neurons are larger than the other neurons for Trojan inputs. This is mainly to activate the target label. For example, the model will not be able to pick up the Trojan if all such neurons activate in the $x < 0$ region of ReLU functions. Based on this, we monitor the activation values of individual neurons, and select the ones that satisfy these two properties.

Specifically, we monitor activation values for individual inputs. For a single input i , we perform a statistical test to see the probability of i activating the Trojan (i.e., blue bars in Fig. 2(a)). In our implementation, we perform the Otsu’s method [38], which is essentially the binary version of Fisher’s linear discriminant analysis, and leverage the Jenks natural breaks optimization algorithm [39] to find the separations of non-linear and linear activation values.

Trojan Unlearning. In detecting hyperplane decision regions, NONE can detect suspicious neurons and inputs whose activation pattern reflect a hyperplane decision region, i.e., the blue bars in Fig. 2(a). Our unlearning then follows a standard machine learning process [40], [41] to eliminate such decision regions and hence, the Trojan. In NONE, we exclude suspicious samples from the training dataset, and also resetting related neurons to a random value to retrain the model. Details of our algorithm can be found in § VIII-D.

Besides this training defense, our theory can also explain and evaluate other training time defenses. We show one example in § VIII-C.

V. EXPERIMENTS

We first introduce the experiment setup (§ V-A). Then, we evaluate the overall effectiveness of NONE (§ V-B) and investigate its robustness against different attack settings (§ V-C). Due to page length limit, impacts of configurable parameters in NONE, generalization on complex applications and potential adaptive attacks are discussed in § VIII.

A. Experiment Setup.

NONE is implemented in Python 3.8 with PyTorch 1.7.0 and CUDA 11.0. If not specified, all experiments are done on a

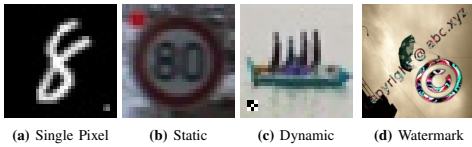


Fig. 3: Examples of Using Different Trigger Patterns.

Ubuntu 18.04 machine equipped with six GeForce RTX 6000 GPUs, 64 CPUs and 376 GB main memory. **Datasets.** We evaluate NONE on five publicly available datasets: MNIST, GTSRB, CIFAR-10, ImageNet-10 and TrojAI (the overview of our datasets is shown in Table VIII and more details are included in § VIII-E.). The default triggers used for each dataset are shown in the last column of Table VIII. And Fig. 3 illustrates poisoned images obtained by patching the original images with different triggers (i.e., a single pixel located in the right bottom corner of Fig. 3(a), a fixed red patch in Fig. 3(b), a black-and-white pattern whose location is random in Fig. 3(c) and a colorful watermark in Fig. 3(d)).

Measurement Metrics. We use benign accuracy (BA) and attack success rate (ASR) [42] as measurement metrics, which is a common practice [43], [34], [23]. BA is defined as the number of correctly classified benign samples over the number of all benign samples. It implies the model’s capability on its original task. ASR is used to evaluate the success rate of Trojan attacks. It is calculated as the number of compromised samples that can successfully attack the model divides the number of all compromised samples.

Models. We evaluate NONE and other defense methods on AlexNet [44], NiN (Network in Network) [16], VGG11, VGG16 [45] and ResNet18 [46]. These models are representative and are commonly used in Trojan related studies [8], [23].

Attack Settings. As we introduced in § II, Trojans are classified into two categories: *Injected Trojans* and *Natural Trojans*. We implement both of them to evaluate NONE and other defense methods. For Injected Trojans, we implement both single target and label specific BadNets [1], label-consistent Trojan attack [10] and hidden trigger Trojan attack [47]. Following the original paper, we use images from a pair of classes (class theater curtain and class plunger) in ImageNet for hidden trigger Trojan attack. For natural Trojans, we follow the previous work [8] to reproduce the attack. Due to the fact that we can not know if the data is poisoned or not in advance, NONE keeps detecting Trojan attacks and training the model even if there is no attack activity. We also evaluate the additional costs of NONE on benign models in non-attack settings. More details for our attack settings are included in § VIII-F.

Comparison. We compare NONE with 4 state-of-the-art defense methods: DP-SGD [21], Neural Attention Distillation (NAD) [31], Activation Clustering (AC) [19] and Anti-backdoor Learning (ABL) [48]. For all compared methods, we use their official code and default hyper-parameters specified in their original papers.

B. Effectiveness of NONE

Experiments. We measure the effectiveness of NONE by comparing the BA and ASR of models protected by NONE with those of undefended models and models protected by existing defenses. The comparison results on injected Trojans, natural Trojans and non-attack settings are shown in Table I, Table II and Table III, respectively. Table I shows the results of defending against injected Trojans. In this table, we show the performance of NONE and comparison results on single-target and label-specific BadNet attacks, Label-consistent attacks and hidden trigger attacks. The detailed defense settings, including attack setup, datasets and network architectures, are shown in each column. For evaluation on natural Trojans, the results are summarized in Table II. The ASR and BA in Table II are the average results under different trigger size settings: 2%, 4%, 6%, 8%, 10% and 12% of the whole image. Notice that, to the best of our knowledge, there is no defense method designed for natural Trojans. We observe that DP-SGD might mitigate natural Trojans because it reduces the high gradients brought from natural Trojans. Therefore, we adapt DP-SGD as the baseline method for natural Trojans. We configure DP-SGD with two settings of parameters from the prior work [21]. For DP-SGD-1, we set the clip as 4.0 and the noise as 0.1. The clip and noise of DP-SGD-2 are 1.0 and 0.5, respectively. Finally, for the non-attack settings, we train several benign models and show the decrease of BA when applying NONE. The results are shown in Table III.

Results on Injected Trojans. From the results on Injected Trojan attacks (Table I), we observe that applying NONE can better protect models from being attacked by injected Trojans. With NONE, the average ASR of models decreases from 93.34% to 1.91%, which is much better than other defense methods (DP-SGD, NAD, AC and ABL can only reduce the average ASR to 30.32%, 34.08%, 45.45% and 68.60% respectively). The reason is that, unlike existing methods based only on specific empirical observations, NONE targets the root cause of the Trojans (i.e., the linearity) and reveals the attacks more accurately.

For the defense cost, we also find that NONE has little negative impact on BA. From Table I, the BA of NONE is the highest among all defense methods and is similar to that of undefended models, meaning that NONE has a low defense cost. The reason is that NONE only modifies the compromised neurons that are highly relevant to Trojan attacks but less related to the original model task. Therefore, most of the benign knowledge is preserved when applying NONE and the model can still perform well on its original tasks. Meanwhile, after the reset process, NONE finetunes the model on the purified data, further strengthening the model capabilities and reducing defense costs.

It is worth clarifying that ABL has a poor performance on label-specific attacks and other attacks that use NiN and VGG models. The possible reason is that the design of ABL requires the model to learn quicker and better on Trojan samples than benign samples [48] (i.e., the learning of malicious

TABLE I: Comparisons on Injected Trojans.

Attack Type	Dataset	Network	Undefended		DP-SGD		NAD		AC		ABL		NONE	
			BA	ASR	BA	ASR	BA	ASR	BA	ASR	BA	ASR	BA	ASR
BadNets (single target)	MNIST	NiN	99.65%	99.96%	92.94%	0.48%	99.26%	0.06%	98.47%	0.51%	98.25%	99.70%	99.58%	0.06%
		VGG11	99.35%	100.00%	97.20%	1.61%	98.85%	2.12%	97.44%	10.93%	98.48%	0.64%	99.11%	0.14%
		ResNet18	99.61%	99.98%	97.31%	0.13%	98.83%	0.12%	98.04%	0.25%	99.34%	0.04%	99.57%	0.37%
	CIFAR-10	NiN	90.52%	100.00%	36.41%	93.01%	80.99%	52.97%	83.77%	100.00%	90.13%	100.00%	90.11%	2.32%
		VGG16	90.46%	100.00%	55.61%	99.32%	88.70%	98.71%	88.14%	99.84%	89.96%	100.00%	89.70%	4.91%
		ResNet18	94.10%	100.00%	52.29%	99.99%	88.74%	1.28%	89.57%	57.43%	92.40%	1.66%	93.62%	1.07%
	GTSRB	NiN	95.95%	99.72%	31.54%	74.78%	96.53%	26.15%	95.36%	99.52%	96.14%	99.54%	95.51%	0.87%
		VGG16	95.43%	99.93%	54.60%	86.83%	95.94%	86.10%	91.28%	5.28%	94.06%	95.79%	94.66%	0.96%
		ResNet18	96.67%	99.84%	55.73%	90.88%	95.95%	13.18%	94.64%	98.57%	96.24%	0.93%	96.39%	0.76%
	ImageNet-10	NiN	82.17%	99.64%	21.22%	65.21%	76.99%	92.61%	74.32%	92.41%	81.35%	99.92%	80.31%	0.14%
		VGG16	88.97%	100.00%	18.06%	44.62%	84.03%	10.93%	81.58%	100.00%	79.16%	100.00%	87.11%	0.14%
		ResNet18	89.83%	99.07%	40.31%	29.58%	86.29%	25.89%	82.39%	98.44%	83.72%	6.83%	86.34%	0.08%
BadNets (label specific)	MNIST	NiN	99.64%	98.86%	93.02%	1.10%	99.24%	0.09%	99.60%	0.03%	98.40%	89.32%	99.42%	0.03%
		VGG11	99.05%	98.99%	97.17%	0.41%	99.06%	32.06%	97.59%	0.10%	99.21%	98.51%	89.63%	0.11%
		ResNet18	99.57%	99.49%	96.81%	0.38%	99.19%	0.19%	99.35%	0.03%	99.01%	98.81%	99.09%	0.20%
	CIFAR-10	NiN	90.50%	78.56%	38.42%	6.43%	82.70%	13.65%	84.74%	56.57%	89.66%	77.69%	89.51%	1.27%
		VGG16	90.73%	96.86%	55.12%	5.23%	88.65%	39.99%	88.18%	82.87%	90.13%	86.91%	89.64%	1.22%
		ResNet18	94.37%	92.00%	52.19%	12.17%	88.21%	1.50%	92.68%	5.29%	83.83%	83.48%	93.05%	1.04%
	GTSRB	NiN	96.06%	93.74%	24.70%	7.39%	96.46%	9.90%	94.02%	6.17%	96.14%	99.54%	95.99%	0.96%
		VGG16	95.71%	94.57%	53.90%	6.71%	96.33%	81.43%	94.96%	69.22%	94.32%	80.21%	95.49%	1.65%
		ResNet18	96.93%	97.40%	60.59%	6.61%	95.49%	11.13%	95.74%	1.16%	90.24%	93.93%	96.63%	0.91%
	ImageNet-10	NiN	82.65%	66.37%	23.44%	10.06%	76.31%	23.31%	78.85%	14.39%	80.20%	56.82%	79.39%	6.98%
		VGG16	89.04%	76.20%	17.94%	10.80%	80.21%	22.17%	81.22%	59.62%	78.34%	53.68%	84.51%	8.31%
		ResNet18	88.87%	59.75%	44.59%	7.95%	85.76%	15.82%	79.44%	23.41%	81.30%	50.52%	84.74%	6.55%
Label consistent	CIFAR-10	NiN	91.32%	98.98%	38.83%	5.21%	82.35%	65.63%	83.92%	95.96%	89.95%	95.28%	90.11%	2.19%
		VGG16	90.97%	98.41%	53.76%	9.24%	88.88%	92.71%	88.88%	7.57%	90.38%	94.94%	90.07%	4.26%
		ResNet18	94.73%	83.42%	54.00%	11.00%	90.74%	60.74%	88.00%	65.86%	87.34%	2.17%	94.01%	2.14%
Hidden Trigger	ImageNet-pair	AlexNet	93.00%	82.00%	80.00%	62.00%	91.00%	74.00%	90.00%	22.00%	90.00%	54.00%	91.00%	4.00%

TABLE II: Comparisons on Natural Trojan.

Dataset	Network	Undefended		DP-SGD-1		DP-SGD-2		NONE	
		BA	ASR	BA	ASR	BA	ASR	BA	ASR
CIFAR-10	NiN	91.02%	87.62%	60.22%	98.85%	39.19%	87.22%	86.94%	34.21%
	VGG11	88.91%	74.00%	77.38%	66.58%	59.26%	62.30%	75.36%	34.03%
	VGG16	90.78%	71.88%	78.25%	61.11%	53.40%	63.58%	81.83%	37.49%
TrojAI	VGG11	99.88%	72.09%	84.51%	88.75%	6.06%	88.55%	99.04%	56.68%
	Resnet18	99.91%	54.33%	78.88%	61.77%	52.81%	58.94%	98.13%	34.98%

TABLE III: Benign Accuracy of Models in Non-attack Settings.

Dataset	Network	Without NONE	With NONE
CIFAR-10	NiN	91.02%	89.40%
	VGG16	90.78%	89.62%
	ResNet18	94.83%	93.92%
GTSRB	NiN	95.68%	95.36%
	VGG16	94.67%	94.08%
	ResNet18	96.89%	96.87%
ImageNet-10	NiN	83.34%	79.18%
	VGG16	88.84%	83.41%
	ResNet18	89.81%	85.25%

training samples should have lower training loss value in the early training stage). When the attacker uses a more complex attack (e.g., label specific BadNets) or a model without very strong learning capabilities (e.g., NiN and VGG), the model is likely cannot learn Trojan tasks quickly and lead to poor performance.

Results on Natural Trojans. From the results in Table II, we find that NONE protects the model most effectively and has lower defense costs against natural Trojans. Overall, com-

pared with DP-SGD methods, which only slightly decreases ASR or even makes ASR larger, applying NONE achieves 1.82 times lower ASR than undefended models. The loss of BA using NONE is also smaller than the loss caused by applying the DP-SGD methods (5.85% with NONE and 35.10% with DP-SGD methods). The results confirm our analysis: reducing the linearity of models significantly reduces the ASR of natural Trojans.

Results on Non-attack Setting. We also explore whether NONE additionally affects benign models' performance on their original tasks. From the result in Table III, we find that NONE has low effect on the BA of benign models (2.33% decrease on average). This is because when there is no Trojan activity, only a few neurons are detected as compromised neurons and are reset by NONE. Moreover, the subsequent training process further reduces the loss of BA. Therefore, we conclude that NONE generally does not impose high additional costs on benign models.

C. Robustness of NONE

We evaluate the robustness of NONE against various attack settings (e.g., different trigger sizes, trigger patterns and poisoning rates). If not specified, the model used in the evaluation is ResNet18. The dataset is CIFAR-10 and the evaluated attack is the single target BadNets attack.

Trigger Sizes. To study the effects of trigger size, we use triggers of different sizes (from 3*3 to 20*20) to attack models and collect their ASR and BA. The experiment results are

TABLE IV: Results on Different Trigger Sizes.

Trigger Size	Undefended		NONE	
	BA	ASR	BA	ASR
3*3	94.10%	100.00%	93.62%	1.07%
5*5	94.27%	100.00%	93.51%	1.34%
7*7	94.10%	99.98%	93.70%	1.53%
9*9	94.34%	100.00%	93.19%	5.18%
15*15	94.44%	100.00%	92.18%	32.27%
20*20	94.58%	100.00%	92.55%	99.82%

TABLE V: Results on Different Trigger Patterns.

Trigger Pattern	Network	Undefended		NONE	
		BA	ASR	BA	ASR
Dynamic Patch	NiN	90.52%	100.00%	90.11%	2.32%
	VGG16	90.46%	100.00%	89.70%	4.91%
	ResNet18	94.10%	100.00%	93.62%	1.07%
Static Patch	NiN	90.92%	100.00%	89.93%	2.61%
	VGG16	90.12%	100.00%	89.48%	4.03%
	ResNet18	94.24%	99.99%	93.93%	1.37%
Watermark	NiN	90.88%	99.99%	87.74%	3.27%
	VGG16	90.64%	99.99%	89.14%	5.36%
	ResNet18	94.28%	100.00%	92.27%	5.99%

shown in Table IV. Overall, the BA of undefended models and models protected by NONE is insensitive to the change in trigger size. The difference between the highest and lowest BA on the unprotected and protected models is 0.48% and 1.52%, respectively, which is very small. We believe that the BA does not change significantly because triggers usually do not interfere with the learning of benign features used for classification, as discussed in previous work [1].

On the other hand, the trigger size affects the ASR of protected models. When the trigger size becomes larger, the ASR of the protected model increases dramatically from 1.07% to 99.82% and NONE fails. The results are understandable because a larger trigger size modifies more pixels in the original image, making the triggers more obvious and easier to learn. As shown in Fig. 10, when the trigger (i.e., black patch in the upper left) is large (i.e., 20*20), it almost covers the whole image (size of the image is 32*32) and becomes the majority of the image. In such a scenario, models easily capture trigger features and are compromised. Currently, the sensitivity to trigger sizes is a common limitation for many defenses [23], [8]. In real applications, considering that a very large trigger size is almost impractical because it makes the trigger too obvious to be detected by the administrator, we still consider NONE is robust to most trigger sizes.

Trigger Patterns. To measure the robustness of NONE against different attack triggers, we use NONE to protect models from being attacked by different triggers. Specifically, we evaluate Dynamic Patch trigger, Static Patch trigger and Watermark trigger on CIFAR-10. The results are shown in Table V. We observe that NONE always achieves low ASR and high BA under different trigger settings. The results demonstrate that NONE is effective against different trigger pattern settings. Moreover, we notice that the ASR of using the watermark trigger is particularly larger compared with

TABLE VI: Results on Different Poisoning Rates.

Poisoning rate	Undefended		NONE	
	BA	ASR	BA	ASR
0.50%	94.46%	100.00%	93.50%	2.52%
5.00%	94.10%	100.00%	93.62%	1.07%
10.00%	93.82%	100.00%	93.13%	1.04%
20.00%	92.70%	100.00%	92.14%	1.39%

using other triggers (i.e., Static Patch and Dynamic Patch). The reason is that the watermark trigger has a larger size and is more complex, as shown in Fig. 3(d).

Poisoning Rates. To measure the impacts of different poisoning rates, we collect the ASR and BA of models being compromised at different poisoning rates from 0.50% to 20.00%. The results are summarized in Table VI. Based on the results, we find that increasing the poisoning rate slightly decreases both the BA and ASR. Specifically, the BA of the model decreases by 1.36% and the ASR of the model decreases by 1.13%. This is because increasing the poisoning rate reduces the number of benign samples used for training, and the BA of the model naturally decreases. Meanwhile, a larger poisoning rate makes compromised samples easier to detect, which leads to a lower ASR. However, in general, the changes in ASR and BA are quite small when attackers use different poisoning rates. Therefore, NONE is considered robust to different poisoning rates.

VI. DISCUSSION

In this paper, we focus the discussion on image classification tasks, which is the focus of many existing works [1], [47], [10], [8], [23], [49]. Expanding our work including the theory and system to other problem domains, such as natural language processing and reinforcement learning, other computer vision tasks, e.g., object detection, will be our future work.

Research on adversarial machines learning potentially have ethical concerns. In this research, we propose a theory to explain existing phenomena and attacks, and propose a new training method which removes Trojans in a DNN model. We believe this is beneficial to the society.

In our current threat model, the adversary can only inject poisoning data into the training dataset, and there does not exist obvious adaptive attacks. However, adaptive adversaries can still conduct attacks under other threat models, and we discuss how this is possible in § VIII-I.

VII. CONCLUSION

In this paper, we present an analysis on DNN Trojans and find relationships between decision regions and Trojans with a formal proof. Moreover, we provide empirical evidence to support our theory. Furthermore, we analyzed the reason why models will have such phenomena is because of linearity of trained layers. Based on this, we propose a novel training method to remove Trojans during training, NONE, which can effectively and efficiently prevent intended and unintended Trojans.

REFERENCES

- [1] T. Gu, B. Dolan-Gavitt, and S. Garg, "Badnets: Identifying vulnerabilities in the machine learning model supply chain," *arXiv preprint arXiv:1708.06733*, 2017.
- [2] J. Jia, Y. Liu, and N. Z. Gong, "Badencoder: Backdoor attacks to pre-trained encoders in self-supervised learning," *arXiv preprint arXiv:2108.00352*, 2021.
- [3] N. Carlini and A. Terzis, "Poisoning and backdooring contrastive learning," *arXiv preprint arXiv:2106.09667*, 2021.
- [4] L. Wang, Z. Javed, X. Wu, W. Guo, X. Xing, and D. Song, "Backdoorl: Backdoor attack against competitive reinforcement learning," *arXiv preprint arXiv:2105.00579*, 2021.
- [5] E. Bagdasaryan and V. Shmatikov, "Spinning sequence-to-sequence models with meta-backdoors," *arXiv preprint arXiv:2107.10443*, 2021.
- [6] X. Chen, A. Salem, M. Backes, S. Ma, and Y. Zhang, "Badnl: Backdoor attacks against nlp models," *arXiv preprint arXiv:2006.01043*, 2020.
- [7] C. Xie, K. Huang, P.-Y. Chen, and B. Li, "Dba: Distributed backdoor attacks against federated learning," in *International Conference on Learning Representations*, 2019.
- [8] Y. Liu, W.-C. Lee, G. Tao, S. Ma, Y. Aafer, and X. Zhang, "Abs: Scanning neural networks for back-doors by artificial brain stimulation," in *Proceedings of the 2019 ACM SIGSAC Conference on Computer and Communications Security*, 2019, pp. 1265–1282.
- [9] X. Chen, C. Liu, B. Li, K. Lu, and D. Song, "Targeted backdoor attacks on deep learning systems using data poisoning," *arXiv preprint arXiv:1712.05526*, 2017.
- [10] A. Turner, D. Tsipras, and A. Madry, "Label-consistent backdoor attacks," *arXiv preprint arXiv:1912.02771*, 2019.
- [11] A. Salem, R. Wen, M. Backes, S. Ma, and Y. Zhang, "Dynamic backdoor attacks against machine learning models," *arXiv preprint arXiv:2003.03675*, 2020.
- [12] A. Nguyen and A. Tran, "Input-aware dynamic backdoor attack," *Advances in Neural Information Processing Systems 30. Pre-proceedings*, 2020.
- [13] D. Tang, X. Wang, H. Tang, and K. Zhang, "Demon in the variant: Statistical analysis of dnns for robust backdoor contamination detection," in *30th USENIX Security Symposium (USENIX Security 21)*, 2021.
- [14] A. Saha, A. Tejankar, S. A. Koohpayegani, and H. Pirsiavash, "Backdoor attacks on self-supervised learning," *arXiv preprint arXiv:2105.10123*, 2021.
- [15] Y. Li, Y. Li, Y. Lv, Y. Jiang, and S.-T. Xia, "Hidden backdoor attack against semantic segmentation models," *arXiv preprint arXiv:2103.04038*, 2021.
- [16] M. Lin, Q. Chen, and S. Yan, "Network in network," *International Conference on Learning Representations*, 2014.
- [17] S. Zhao, X. Ma, Y. Wang, J. Bailey, B. Li, and Y.-G. Jiang, "What do deep nets learn? class-wise patterns revealed in the input space," *arXiv preprint arXiv:2101.06898*, 2021.
- [18] B. Tran, J. Li, and A. Madry, "Spectral signatures in backdoor attacks," *arXiv preprint arXiv:1811.00636*, 2018.
- [19] B. Chen, W. Carvalho, N. Baracaldo, H. Ludwig, B. Edwards, T. Lee, I. Molloy, and B. Srivastava, "Detecting backdoor attacks on deep neural networks by activation clustering," *SafeAI@AAAI*, 2019.
- [20] M. Du, R. Jia, and D. Song, "Robust anomaly detection and backdoor attack detection via differential privacy," *International Conference on Learning Representations*, 2020.
- [21] S. Hong, V. Chandrasekaran, Y. Kaya, T. Dumitras, and N. Papernot, "On the effectiveness of mitigating data poisoning attacks with gradient shaping," *arXiv preprint arXiv:2002.11497*, 2020.
- [22] M. Abadi, A. Chu, I. Goodfellow, H. B. McMahan, I. Mironov, K. Talwar, and L. Zhang, "Deep learning with differential privacy," in *Proceedings of the 2016 ACM SIGSAC conference on computer and communications security*, 2016, pp. 308–318.
- [23] B. Wang, Y. Yao, S. Shan, H. Li, B. Viswanath, H. Zheng, and B. Y. Zhao, "Neural cleanse: Identifying and mitigating backdoor attacks in neural networks," in *2019 IEEE Symposium on Security and Privacy (SP)*. IEEE, 2019, pp. 707–723.
- [24] X. Xu, Q. Wang, H. Li, N. Borisov, C. A. Gunter, and B. Li, "Detecting ai trojans using meta neural analysis," *arXiv preprint arXiv:1910.03137*, 2019.
- [25] S. Kolouri, A. Saha, H. Pirsiavash, and H. Hoffmann, "Universal litmus patterns: Revealing backdoor attacks in cnns," in *Proceedings of the IEEE/CVF Conference on Computer Vision and Pattern Recognition*, 2020, pp. 301–310.
- [26] S. Huang, W. Peng, Z. Jia, and Z. Tu, "One-pixel signature: Characterizing cnn models for backdoor detection," in *European Conference on Computer Vision*. Springer, 2020, pp. 326–341.
- [27] W. Guo, L. Wang, X. Xing, M. Du, and D. Song, "Tabor: A highly accurate approach to inspecting and restoring trojan backdoors in ai systems," *IEEE International Conference on Data Mining (ICDM)*, 2020.
- [28] G. Shen, Y. Liu, G. Tao, S. An, Q. Xu, S. Cheng, S. Ma, and X. Zhang, "Backdoor scanning for deep neural networks through k-arm optimization," *arXiv preprint arXiv:2102.05123*, 2021.
- [29] K. Liu, B. Dolan-Gavitt, and S. Garg, "Fine-pruning: Defending against backdooring attacks on deep neural networks," in *International Symposium on Research in Attacks, Intrusions, and Defenses*. Springer, 2018, pp. 273–294.
- [30] P. Zhao, P.-Y. Chen, P. Das, K. N. Ramamurthy, and X. Lin, "Bridging mode connectivity in loss landscapes and adversarial robustness," *arXiv preprint arXiv:2005.00060*, 2020.
- [31] Y. Li, N. Koren, L. Lyu, X. Lyu, B. Li, and X. Ma, "Neural attention distillation: Erasing backdoor triggers from deep neural networks," *International Conference on Learning Representations*, 2021.
- [32] D. Wu and Y. Wang, "Adversarial neuron pruning purifies backdoored deep models," *Advances in Neural Information Processing Systems*, vol. 34, 2021.
- [33] Y. Zeng, S. Chen, W. Park, Z. M. Mao, M. Jin, and R. Jia, "Adversarial unlearning of backdoors via implicit hypergradient," *arXiv preprint arXiv:2110.03735*, 2021.
- [34] Y. Gao, C. Xu, D. Wang, S. Chen, D. C. Ranasinghe, and S. Nepal, "Strip: A defence against trojan attacks on deep neural networks," in *Proceedings of the 35th Annual Computer Security Applications Conference*, 2019, pp. 113–125.
- [35] E. Chou, F. Tramèr, and G. Pellegrino, "Sentinet: Detecting localized universal attacks against deep learning systems," in *2020 IEEE Security and Privacy Workshops (SPW)*. IEEE, 2020, pp. 48–54.
- [36] I. J. Goodfellow, J. Shlens, and C. Szegedy, "Explaining and harnessing adversarial examples," *International Conference on Learning Representations*, 2015.
- [37] R. Tang, M. Du, N. Liu, F. Yang, and X. Hu, "An embarrassingly simple approach for trojan attack in deep neural networks," in *Proceedings of the 26th ACM SIGKDD International Conference on Knowledge Discovery & Data Mining*, 2020, pp. 218–228.
- [38] N. Otsu, "A threshold selection method from gray-level histograms," *IEEE transactions on systems, man, and cybernetics*, vol. 9, no. 1, pp. 62–66, 1979.
- [39] G. F. Jenks, "Optimal data classification for choropleth maps," *Department of Geography, University of Kansas Occasional Paper*, 1977.
- [40] L. Bourtole, V. Chandrasekaran, C. A. Choquette-Choo, H. Jia, A. Travers, B. Zhang, D. Lie, and N. Papernot, "Machine unlearning," *arXiv preprint arXiv:1912.03817*, 2019.
- [41] Y. Cao and J. Yang, "Towards making systems forget with machine unlearning," in *2015 IEEE Symposium on Security and Privacy*. IEEE, 2015, pp. 463–480.
- [42] A. K. Veldanda, K. Liu, B. Tan, P. Krishnamurthy, F. Khorrami, R. Karri, B. Dolan-Gavitt, and S. Garg, "Nnoctation: broad spectrum and targeted treatment of backdoored dnns," *arXiv preprint arXiv:2002.08313*, 2020.
- [43] B. G. Doan, E. Abbasnejad, and D. C. Ranasinghe, "Februus: Input purification defense against trojan attacks on deep neural network systems," in *Annual Computer Security Applications Conference*, 2020, pp. 897–912.
- [44] A. Krizhevsky, I. Sutskever, and G. E. Hinton, "Imagenet classification with deep convolutional neural networks," *Advances in neural information processing systems*, vol. 25, pp. 1097–1105, 2012.
- [45] K. Simonyan and A. Zisserman, "Very deep convolutional networks for large-scale image recognition," *arXiv preprint arXiv:1409.1556*, 2014.
- [46] K. He, X. Zhang, S. Ren, and J. Sun, "Deep residual learning for image recognition," in *Proceedings of the IEEE conference on computer vision and pattern recognition*, 2016, pp. 770–778.
- [47] A. Saha, A. Subramanya, and H. Pirsiavash, "Hidden trigger backdoor attacks," in *Proceedings of the AAAI Conference on Artificial Intelligence*, vol. 34, no. 07, 2020, pp. 11957–11965.

- [48] Y. Li, X. Lyu, N. Koren, L. Lyu, B. Li, and X. Ma, "Anti-backdoor learning: Training clean models on poisoned data," *Advances in Neural Information Processing Systems*, vol. 34, 2021.
- [49] E. Bagdasaryan and V. Shmatikov, "Blind backdoors in deep learning models," in *30th USENIX Security Symposium (USENIX Security 21)*, 2021, pp. 1505–1521.
- [50] J. Bai, B. Wu, Y. Zhang, Y. Li, Z. Li, and S.-T. Xia, "Targeted attack against deep neural networks via flipping limited weight bits," *arXiv preprint arXiv:2102.10496*, 2021.
- [51] V. Nair and G. E. Hinton, "Rectified linear units improve restricted boltzmann machines," in *Icml*, 2010.
- [52] A. L. Maas, A. Y. Hannun, and A. Y. Ng, "Rectifier nonlinearities improve neural network acoustic models," in *Proc. icml*, vol. 30, no. 1. Citeseer, 2013, p. 3.
- [53] D.-A. Clevert, T. Unterthiner, and S. Hochreiter, "Fast and accurate deep network learning by exponential linear units (elus)," *arXiv preprint arXiv:1511.07289*, 2015.
- [54] "Tanhshrink," <https://pytorch.org/docs/stable/generated/torch.nn.Tanhshrink.html>.
- [55] H. Zheng, Z. Yang, W. Liu, J. Liang, and Y. Li, "Improving deep neural networks using softplus units," in *2015 International Joint Conference on Neural Networks (IJCNN)*. IEEE, 2015, pp. 1–4.
- [56] N. Tursynbek, A. Petiushko, and I. Oseledets, "Robustness threats of differential privacy," *arXiv preprint arXiv:2012.07828*, 2020.
- [57] S.-M. Moosavi-Dezfooli, A. Fawzi, J. Uesato, and P. Frossard, "Robustness via curvature regularization, and vice versa," in *Proceedings of the IEEE/CVF Conference on Computer Vision and Pattern Recognition*, 2019, pp. 9078–9086.
- [58] Y. LeCun, L. Bottou, Y. Bengio, and P. Haffner, "Gradient-based learning applied to document recognition," *Proceedings of the IEEE*, vol. 86, no. 11, pp. 2278–2324, 1998.
- [59] J. Stallkamp, M. Schlipsing, J. Salmen, and C. Igel, "Man vs. computer: Benchmarking machine learning algorithms for traffic sign recognition," *Neural networks*, vol. 32, pp. 323–332, 2012.
- [60] A. Geiger, P. Lenz, C. Stiller, and R. Urtasun, "Vision meets robotics: The kitti dataset," *The International Journal of Robotics Research*, vol. 32, no. 11, pp. 1231–1237, 2013.
- [61] A. Krizhevsky, G. Hinton *et al.*, "Learning multiple layers of features from tiny images," 2009.

VIII. APPENDIX

Roadmap: We demonstrate empirical results of relaxations (§ VIII-A), more empirical evidence for model’s linearity (§ VIII-B), explanation for DP-SGD (§ VIII-C) and a detailed NONE defense algorithm (§ VIII-D). Then, we provide implementation details including details of datasets (§ VIII-E) and used attacks (§ VIII-F). We also measure the sensitivity of NONE against different configurable parameters (§ VIII-G) and the generalization on real-world applications (§ VIII-H). Finally, we evaluate NONE on an adaptive attack (§ VIII-I).

A. Empirical Evidence for § III-A

To evaluate if the Trojan decision region in real world data is the relaxation of the Trojan linear hyperplane (§ III-A), we visualize the decision regions of Trojane neural networks.

Following Bai et al. [50], we visualize the decision region of neural networks on 2d data. Specifically, We visualize decision regions of compromised Multilayer Perceptrons (MLP) trained on different poisoning rates. The MLP model has 5 layers and each layer contains 100 neurons, and we use ReLU as the activation function. Similar to Bai et al. [50], the used dataset contains five isotropic Gaussian 2d blobs, in which each blob represents a class. In Fig. 6, we show the complete and accurate Trojan decision region (Fig. 6(a)) for this model and real-world relaxations with different poisoning rates of BadNets attack (Fig. 6(b), Fig. 6(c), Fig. 6(d)). Each color

in the figure denotes one output label. In our experiments, we set the trigger to $t = (-, 0.6)$, and the target class $y_t = 3$ (red). Thus, the red region close to $t = (-, 0.6)$ denotes the Trojan region. We observe that, with the growth of poisoning ratio, the attacks get a higher attack success rate and become more accurate, and the Trojan region also converts to the ideal one shown in Fig. 6(a). Despite such relaxations, we can also confirm that the Trojan region has a large intersection with the hyperplane and other possible triggers are around the ground truth one.

B. More Empirical Evidence for § III-B

Different model architectures. To evaluate the linearity on different model architectures, we collect the activation outputs of models with different architectures (i.e., NiN and VGG16). Similar to § III-B, we use both benign samples and compromised samples as the input of models, and collect their activation outputs. The results are shown in Fig. 4. The results show that compromised samples always lead to significantly higher activation values than benign samples in different models. The conclusion is consistent with the linearity theory in § III and proves that our theory can generalize on different model architectures.

Different model layers: Besides the linearity on different model architectures, we also evaluate the linearity on different model layers. Fig. 5 demonstrates the activation outputs of different convolutional layers (i.e., 14th to 17th layers). Note that we only show the results on 4 layers due to the space limitation. The results on other layers are similar. From the results, we observe that Trojans introduce a large set of high activation values in each layer, leading to the final linearity between input and activation output. The results are consistent with our previous analysis in § III and further confirm that Trojans can introduce linearity at each layer of the DNN model.

Different activation functions. To investigate if our theory and NONE can generalize on different activation functions, we train 5 ResNet18 models on CIFAR-10 with 2 common used linear activation functions (i.e., ReLU [51], LeakyReLU [52]) and 3 non-linear activation functions (i.e., ELU [53], Tanhshrink [54] and Softplus [55]). Then we apply NONE to protect these models. We report the ASR and BA of both protected models and undefended models. The results are shown in Table VII. Overall, we find that NONE always achieves a low ASR when using different activation functions, showing the generalization of NONE on different activation functions. Even with non-linear activation functions, NONE is still effective and we suspect the reason is that even though some activation functions are non-linear, well-trained deep neural networks do fall into the "highly linear" regions. The results are also consistent with existing papers [36].

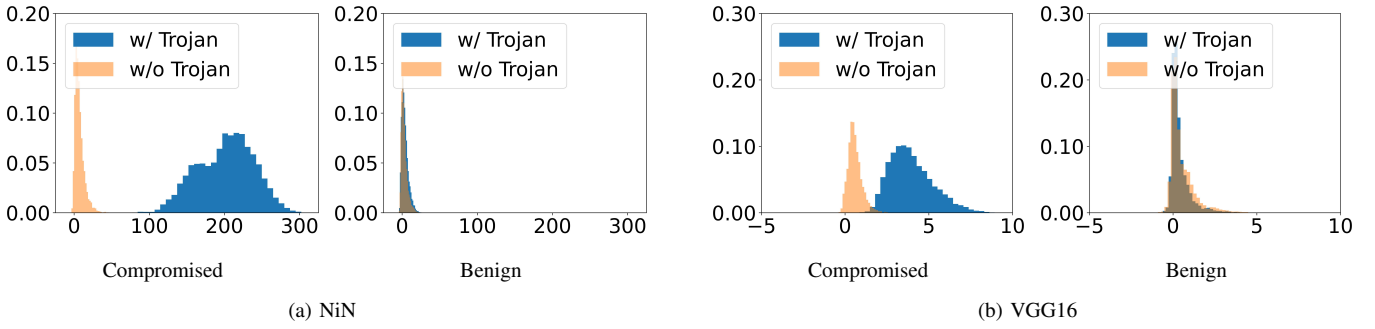


Fig. 4: Comparison of Activation Values on Different Network Architectures.

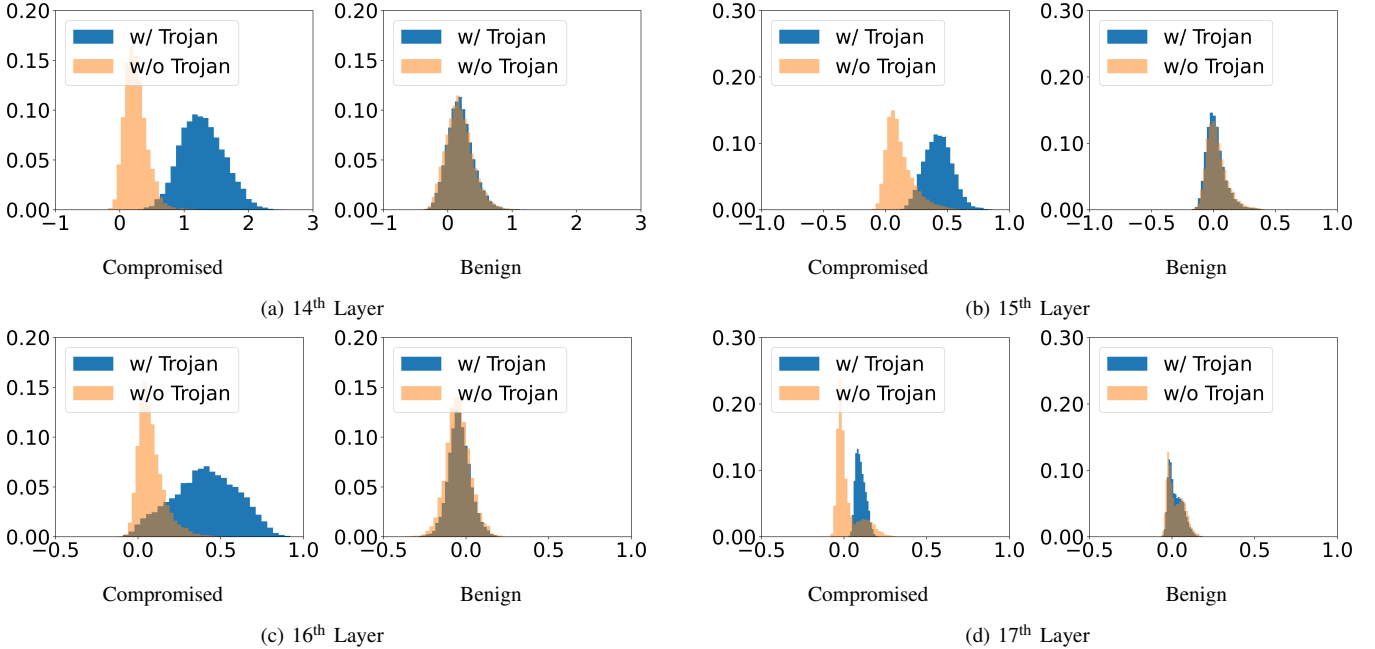


Fig. 5: Comparison of Activation Values on Different CNN Layers in ResNet18 Model.

TABLE VII: Evaluation Results with Different Activation Functions.

Activation Function	Undefended		NONE	
	BA	ASR	BA	ASR
ReLU	94.10%	100.00%	93.62%	1.07%
LeakyReLU	94.32%	100.00%	93.48%	1.24%
ELU	92.99%	99.93%	91.11%	1.46%
Tanhshrink	91.68%	99.76%	90.18%	5.11%
Softplus	92.81%	100.00%	89.91%	2.07%

C. Explaining DP-SGD Defense

DP-SGD [21] improves existing SGD methods by removing the noises added to poisoning training samples and shadows promising results in defending against Trojans. Here, we explain why it works. Specifically, we use the same settings with Fig. 6 to train 2 compromised models with vanilla SGD and DP-SGD, and show the comparison results in Fig. 7. Results show that data poisoning can successfully attack the vanilla SGD method. As a comparison, DP-SGD makes the decision region (red) much more complex, and removes the malicious “hyperplane” effects to defense against Trojans.

Recently, Tursynbek et al. [56] quantitatively measured the curvature of DNN using Curvature Profile [57] and showed that models trained with DP-SGD produce more curved decision boundaries, which is consistent with our results. By doing so, DP-SGD breaks the “hyperplane” Trojans rely on and hence, removes the Trojan effects. However, this unavoidably affects the accuracy of benign samples. As shown in Fig. 7, many benign samples got misclassified.

D. Detailed NONE Defense Algorithm

Based on our analysis in § III-B, we know that Trojans are related to linear activation values in layers. When they are linear, the learned DNN form a Trojan decision region, based on relaxations of Theorem III.5. To solve this issue, we propose Algorithm 1 to enforce non-linearity in individual layers by resetting potentially linear neurons and remove data samples that cause such linearity. This is a revised training process, which essentially is an iterative process that trains the model till the maximal epochs (line 2). It starts by training the model using standard backward propagation method (line

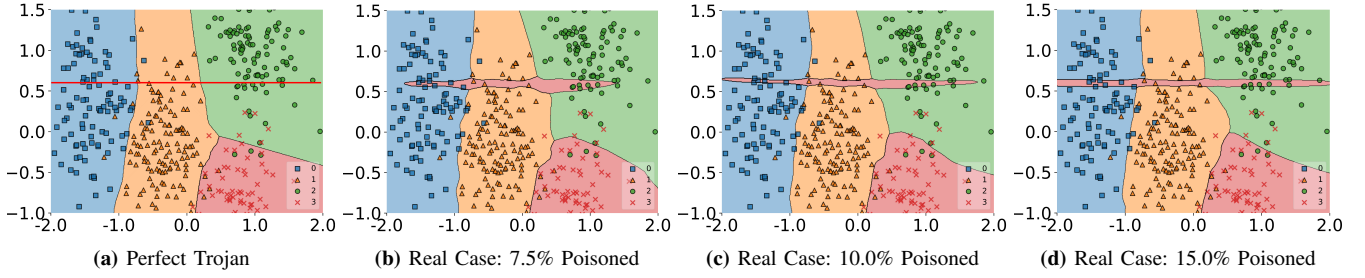


Fig. 6: Perfect Trojans and Relaxations on 2D Data. Each sub-figure contains test samples (dots) and the learned decision regions for different labels (in different colors) under a specific setting. The Trojan trigger is $t = (-, 0.6)$, and the target label $y_t = 3$. The red region near $(-, 0.6)$ is the learned Trojan decision region.

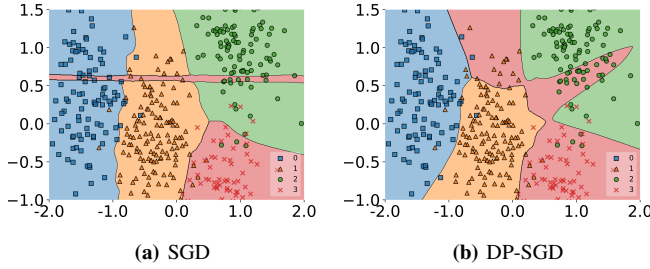


Fig. 7: Decision Region Generated by SGD and DP-SGD.

4). During training, we also gather all activation values of individual neurons A for all training samples in training dataset D . Then, the process contains three steps: identifying compromised neurons (lines 6 to 10), identifying biased or poisoning samples (lines 11 to 17) and lastly resetting the neurons for retraining (lines 18 to 20). The first step is to identify comprised neurons, namely the neurons that carry Trojans. Based on our discussion on § III-B, we do this by checking the activation values of neuron n , denoted as A_n , to see if its function is highly linear using the condition $\mathbb{P}(A_n \geq 0) \geq \theta$. If so, we make the neuron n as potentially compromised and add it to the candidate set C . The second step is to identify highly biased samples or poisoning samples. The overall design is a statistical testing process: we first find a reference distribution of a particular neuron that represent its benign activation values, and then mark all inputs whose activation values do not follow such distributions as potentially biased or poisoning samples. The idea of finding a benign distribution is that inputs whose activation values in a layer is non-linear are considered as benign and the distribution that describes the activation values of these inputs is used as the reference distribution. In Algorithm 1, line 13 uses a function to test the linearity of activation values and separate all activation values into a benign set B and others O . Then, we normalize the distribution of our reference distribution B to a normal distribution and obtain its mean value μ and standard deviation value σ (line 14). For a single input i , we perform a statistical test to see the probability of i being a potentially biased or poisoning sample (line 15 to 16). Following standard convention, we use $\lambda = 3$ indicating that 95% of cases should

Algorithm 1 Training

Input: Training Data: D , Maximal epoch: E

Output: Model: M

```

1: function TRAINING( $D$ )
2:   while  $e \leq E$  and (not terminate( $M$ )) do
3:      $\triangleright$  Train and gather activation values
4:      $M = \text{train}(D, e)$ 
5:      $A = M.\text{predict}(D)$ 
6:      $\triangleright$  Identify compromised neurons
7:      $C = \emptyset$ 
8:     for neuron  $n$  in  $M$  do
9:       if  $\mathbb{P}(A_n \geq 0) \geq \theta$  then
10:         $C = C \cup \{n\}$ 
11:     $\triangleright$  Identify biased or poisoning samples
12:    for neuron  $n \in C$  do
13:       $B_n, O_n = \text{separate}(A_n)$ 
14:       $\mu, \sigma = \text{norm}(B_n)$ 
15:      for activation value of input  $i : i_n \in O_n$  do
16:        if  $\left| \frac{i_n - \mu}{\sigma} \right| \geq \lambda$  then
17:           $D = D - i$ 
18:     $\triangleright$  Resetting compromised neurons
19:    for neuron  $c \in C$  do
20:       $c = M.\text{init}(c)$ 

```

fall in this range. Values out of this range are highly likely abnormal. If so, we exclude it from the training dataset (line 17). The last step of our training algorithm is to remove the compromised neuron effects from the model by resetting them. For all identified compromised neurons, we reuse the initialization method in our training setting to set a new value for them (line 19 and 20). Then, we continue the training until terminating conditions are met or the training budget is used up (line 2).

This algorithm uses ReLU as an example, and because our theory still holds for other activation functions (see § VIII-B), the algorithm can generalize to other models by modifying corresponding parameters (line 9). To identify compromised neurons and biased/poisoning images, we need to determine the threshold value θ (line 8) and separate the activation values to non-linear and linear ones. In our implementation, we perform the Fisher’s linear discriminant analysis (its binary

version, Otsu’s method [38]) and leverage the Jenks natural breaks optimization algorithm to find the separations of non-linear and linear activation values. Sets B and O are outputs of such algorithms, and we use the standard value that evaluates the quality of such separation to compute the value of our threshold θ , i.e., 0.95 in our case. Notice such values can affect the accuracy of identifying compromised neurons and inputs. To evaluate our approach, we also choose other alternative ways of separating the sets and present the results in § VIII-G.

Similar to model pruning and fine-tuning, when we reset different number of neurons (line 19 and 20), the accuracy on benign and Trojan samples can be different. To evaluate the sensitivity of NONE on different number of neurons to reset during training and identify malicious samples, we introduce two parameters, r_1 represents the fraction of neurons to be reset and r_2 denotes the fraction of neurons that are used in identifying malicious samples. We rank all neurons and inputs and only choose the top r_1 or r_2 percent to be included in our following operations. In § VIII-G (i.e., Resetting Fraction, Selection Threshold), we use different values of r_1 and r_2 to understand how they affect the system.

E. Dataset Details

The overview of the dataset is shown in Table VIII. Specifically, we order the datasets with their data sizes and show their dataset names, input size of each sample, the total number of samples, the number of classes and the default Trojan triggers used for generating poisoned data in each column. Among these datasets, MNIST¹ [58] is widely used for digit classification tasks. The GTSRB² [59] dataset is used for traffic sign recognition tasks in the self-driving scenario. TrojAI³ contains the images created by compositing a synthetic traffic sign, with a random background image from the KITTI dataset [60]. Other datasets (i.e., CIFAR-10⁴ [61] and ImageNet-10⁵ [44]) are built for recognizing general objects (e.g., animals, plants and handicrafts). The default triggers (Fig. 3) used for each dataset are shown in the last column of Table VIII.

F. Attack Details

We first evaluate the performances of NONE against Bad-Nets on two different settings: single target attack and label specific attack. [1] For the single target attack, we set the label whose index is 0, 0, 1 and 1 as the predefined target label for MNIST, CIFAR-10, GTSRB and ImageNet-10 datasets, respectively. For label specific attack, the target label of each sample is the label whose index is (the label index of this sample plus 1)%(the number of classes in the dataset). Then, we evaluate the defense against the label-consistent attack and the natural Trojan attack. We use the same implementation and parameters in previous works [10], [8] to achieve these attacks and compare NONE with other defense methods.

¹<http://yann.lecun.com/exdb/mnist/>

²https://benchmark.ini.rub.de/gtsrb_news.html

³<https://pages.nist.gov/trojAI/>

⁴<https://www.cs.toronto.edu/~kriz/cifar.html>

⁵<https://github.com/fastai/imagenette>

TABLE VIII: Overview of Datasets.

Name	Input Size	Samples	Classes	Trigger
MNIST	28*28*1	60000	10	Single Pixel
GTSRB	32*32*3	39209	43	Static
CIFAR-10	32*32*3	50000	10	Dynamic
ImageNet-10	224*224*3	9469	10	Watermark
TrojAI	224*224*3	125000	5-25	Natural Trojans

Notice that for the label-consistent attack, the official github repository⁶ only provides poisoned CIFAR-10 datasets, and the code for training GAN and generating poisoned samples are not released. Therefore, we only evaluate NONE on CIFAR-10. For defending against the hidden trigger Trojan attack, we follow the parameter settings in the previous work [47] and use a pair of image categories (i.e., randomly selected from ImageNet dataset in the previous work [47]) for testing.

G. Sensitivity to Configurable Parameters

NONE has a few configurable parameters that may affect its performance: learning rate in training, resetting fraction, number of neurons in each layer used to detect malicious samples (selection threshold) and different thresholds used for the identification of compromised neurons. We vary the configurable parameters in NONE independently and evaluate the impact of each. The setting of dataset, models and attack type is the same as evaluation in § V-C. We use 5% poisoning rate, 3*3 trigger size as the default attack setting.

Learning Rate in Training. Learning rate usually affects the accuracy and convergence speed of the model during the training process. To understand how the learning rate impacts the model deployed with NONE, we choose learning rates from 0.01 to 0.00001 and then measure the BA and ASR of models using different learning rates in the training process. The results are shown in Fig. 8.

Overall, as shown in Fig. 8(a), using a larger learning rate makes the convergence process faster and the BA lower, except for using the learning rate 0.01. This is because using a larger learning rate can update the weights quickly, but a too large learning rate makes it difficult to find the local optimum and decrease the BA.

In addition, in Fig. 8(b), we find that the final ASR is decreased with the decrease of learning rate after the model is converged. Using learning rate 0.00001 finally achieves the lowest ASR. The reason is that increasing the learning rate tends to make the model skip the local optimal value and get a more likely worse value.

Therefore, combining the results in these 2 subfigures, we choose the learning rate 0.001 as the default setting in § V-B because using 0.001 achieves the best BA and ASR. The epoch number is set to 5 because ASR is not decreased after 5 epochs and the BA is already good.

Resetting Fraction. Resetting fraction (i.e., r_1 in § VIII-D) measures the number of neurons that are reset by NONE. Specifically, NONE first sorts the probabilities that the neuron has activation values larger than 0 and then resets the

⁶<https://github.com/MadryLab/label-consistent-backdoor-code>

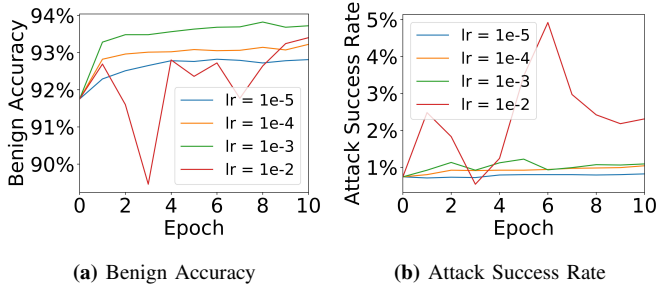


Fig. 8: Evaluation Results with Different Learning Rates.

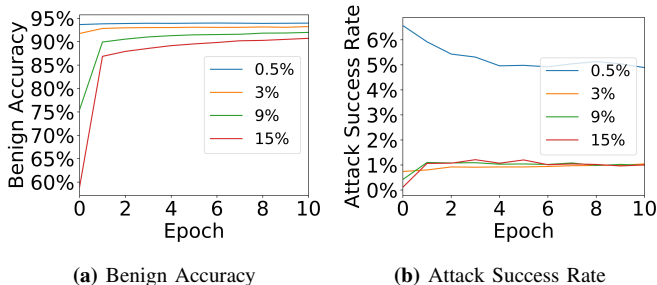


Fig. 9: Evaluation Results with Different Resetting Fractions.

neurons whose probabilities is in top $r_1\%$ in each layer. Using a smaller resetting fraction makes NONE to detect compromised neurons more conservatively (only labeling and resetting the most likely compromised neurons). To measure the effect of resetting fraction on defense performance of NONE, we obtain the BA and ASR of models at different resetting fractions from 0.5% to 15%. The results are shown in Fig. 9, where the legend shows different resetting fraction values.

From the results in Fig. 9(a), it is obvious that when we use a larger resetting fraction and reset more neurons, the final BA is lower. The reason is that after we reset neurons, some good features learned by the model are lost, which decreases the final BA. When we reset more neurons (i.e., using a larger resetting fraction), the model loses more high quality features and decreases more BA. Therefore, to avoid losing too much BA, the resetting fraction is recommended to be small.

Furthermore, in Fig. 9(b), we find that different resetting fractions do not affect the ASR of models after a certain threshold (i.e., 3%). Because when the resetting fraction is large, NONE can successfully detect almost all compromised neurons. Increasing the resetting fraction does not help NONE to detect more compromised neurons.

Based on the above conclusions, we set the default resetting fraction as 3% because using resetting fraction 3% requires changing fewer neurons, achieving high BA and low ASR.

Selection Threshold. When detecting poisoning samples, we only use the neurons whose compromised values are larger than the values of a portion of neurons in the same layer and we call this portion as selection threshold (i.e., r_2 in § VIII-D). To fully understand the impact of this threshold, we vary the threshold from 1 neuron to 100% neurons in the dataset and

TABLE IX: Results on Different Selection Thresholds.

Number of Neurons	Single Target Attack		Label Specific Attack	
	BA	ASR	BA	ASR
top 1	93.11%	1.03%	93.31%	0.96%
top 0.5%	93.10%	1.07%	93.32%	0.96%
top 1%	93.13%	1.07%	93.37%	0.95%
top 10%	93.11%	1.06%	93.29%	1.04%
top 30%	93.14%	1.04%	93.26%	41.07%
top 50%	93.08%	1.04%	93.18%	60.12%
top 100%	93.05%	1.07%	93.14%	71.78%

collect the corresponding BA and ASR under different attack settings. We test the single target BadNets attack and the label specific BadNets attack. We then show the results in Table IX, where the first column shows the threshold and the following columns show the results against the BadNets.

As the results show, when we increase the selection threshold, the ASR of the label specific BadNets attack significantly increases when the threshold is larger than 10%. This is because only a few neurons in the model are compromised. If the selection threshold is larger than the number of compromised neurons, NONE chooses many benign neurons to identify whether a sample is malicious or not, which introduces more noise and reduces the detection accuracy because benign neurons are not sensitive to Trojan behavior. Furthermore, the label specific BadNets attack specifies many different labels as target labels, making the attack stealthy and detecting the attack more difficult. Therefore, with the increase of the selection threshold, the defense performance becomes worse.

However, we observe that the ASR of the single target standard Trojan attack is not correlated with the selection threshold, showing the robustness of NONE to selection threshold against the single target Trojan attack. This is due to the fact that the single target BadNets attack only focuses on one label, making the malicious behavior more obvious, thus reducing the impact of introduced noise and still achieving a low ASR.

For the BA, we find that the BA against both the single target BadNets attack and the label specific BadNets attack is stable. Although using a lower selection threshold may allow NONE to filter out malicious samples conservatively (i.e., only use the most likely compromised neurons to detect malicious samples), enabling NONE to train the model on most of the data and achieve good BA results. Choosing a higher selection threshold does not decrease the BA significantly. Because considering there are a large number of benign samples in the dataset, even a higher selection threshold introduces more benign neurons (i.e., noise) to identify malicious samples and reduces the number of benign samples for finetuning, NONE still has enough benign samples for training and achieves similar BA results as using low selection thresholds.

Therefore, considering both BA and ASR, we set the selection threshold as 10% to avoid the ASR increasing significantly.

Parameters in Compromised Neurons Identification. As mentioned in § VIII-D, we use an alternative implementation to evaluate our design. We first obtain two clusters of samples

TABLE X: Results on Different λ_l and λ_h .

λ_h	BA	ASR	λ_l	BA	ASR
0.3	93.22%	1.07%	0.1	93.18%	1.13%
0.5	93.05%	1.14%	0.3	93.08%	0.99%
0.7	93.13%	1.11%	0.5	93.18%	1.11%
0.9	93.12%	1.11%	0.7	93.11%	1.03%

TABLE XI: Results on Federated Learning.

Dataset	Undefended		NONE	
	BA	ASR	BA	ASR
MNIST	99.22%	99.15%	98.60%	0.13%
CIFAR-10	80.31%	43.23%	78.67%	4.44%

according to their final layer probability outputs (the value in the probability vector). Subsequently, we classify the samples whose probability values are lower than a threshold λ_l to the first cluster (i.e., low confidence samples) and classify the samples whose probability values are higher than λ_h to the second cluster (i.e., low confidence samples). Then, we use the gap between two clusters to measure the linearity of each neuron. If a neuron has high linearity (i.e., top r_1 in a layer), then we consider it as a compromised neuron. In this process, λ_h and λ_l determine the selection of the high confidence samples and the low confidence samples that affect the defense performance of NONE. Therefore, to fully understand the impacts of them, We vary λ_h and λ_l values, and obtain the corresponding ASR and BA. By default, we use λ_h as 0.9 and λ_l to be 0.1 when the other parameter is changing.

Table X shows the results with different λ_h and λ_l settings. The results indicate that there is no obvious correlation between the performance of NONE and parameters (i.e., λ_l and λ_h). As the results show, the ASR of models is always around 1.11% under different parameter settings. And the difference between the highest BA and the lowest BA is 0.17% which is quite small. Therefore, NONE is not sensitive to λ_l and λ_h , which improves the usability of NONE.

H. Generalization on complex applications

Attackers may conduct attacks in a more complex scenario. To measure the generalization of NONE on complex applications, we evaluate NONE on 2 federated learning applications trained on different datasets (i.e., MNIST and CIFAR-10) and a transfer learning application. Each federated learning application has 10 participants, in which 4 of them are malicious participants who conduct the distributed Trojan attacks [7] jointly to inject Trojan triggers into the global model. We assume that attackers train their local models on the poisoned training data and contribute to the global model without scaling the original weight of the poisoned local models. We then apply NONE on the global model to defend against the Trojan attack from malicious local models. Specifically, NONE requires the participants use their data to test the global model and upload the activation values of the global model to identify compromised neurons. To measure the defense performance, we measure the BA and ASR of the global models (i.e., the original model and model deployed

**Fig. 10:** Trojan Inputs with Large Triggers.

with NONE). The results are shown in Table XI. As shown in the table, on average, NONE achieve 31.16 times lower ASR than undefended models with a slight decrease (i.e., 1.13%) in the BA. The results show that NONE can defend against the Trojan attacks effectively in real-world federated learning applications with a low cost. Besides federated learning, we have also discussed the performance of NONE in transfer learning settings. Hidden Trigger Trojan Attack [47] in § V-B is conducted in transfer learning scenarios and the results are shown in Table I. As the results show, NONE achieves low ASR (i.e., 4.00%) and high BA (i.e., only 2.00% lower than undefended models), proving the generalization of NONE on transfer learning settings.

I. Adaptive Attack.

For adaptive attackers, their goal is to train a Trojaned model with low linearity and try to evade the defense of NONE. However, under our threat model, the adversary can only poison the data but cannot modify the training process of NONE, which makes reducing the model’s internal linearity almost impossible. Therefore, we relax the threat model for attackers and allow the attacker to control the training process of the model. We also assume the defender can access both the training data and the trained model. The defender tries to use NONE to eliminate Trojans injected in the model trained by the attacker.

Then, we design an adaptive loss that minimizes the activation difference between benign samples and corresponding Trojan samples to achieve attack goals. The adaptive loss is defined in Eq. 9, where x is benign sample and \tilde{x} is the corresponding Trojan sample (i.e., the sample obtained by pasting trigger on x). y and y_t are the label of benign sample x and target label respectively. F_θ donates the final prediction of the model. \mathcal{L} means the Cross-Entropy criterion. Meanwhile, I_i is the feature on the i -th layer, and α is the weight that control the influence of the third loss item. By design, the loss function minimizes the distance between activation values of benign samples and the corresponding Trojan samples, making the Trojan decision region more curve and complex. Trojaned models trained with the adaptive loss should have low linearity and may evade the detection of NONE.

$$\mathcal{L}(F_\theta(x), y) + \mathcal{L}(F_\theta(\tilde{x}), y_t) + \alpha \sum (I_i(x) - I_i(\tilde{x}))^2 \quad (9)$$

To measure whether the adaptive attack works, we first train a benign model and then fine-tune that model using adaptive loss when attackers use poisoned data to attack the model. The Trojan trigger we use in the attack is the watermarking trigger and the model is VGG16. The results are shown in Table XII. The results show that NONE does not always

TABLE XII: Adaptive Attack.

α	Undefended		NONE	
	BA	ASR	BA	ASR
1e-4	90.06%	100.00%	88.48%	67.89%
1e-3	89.53%	99.97%	87.92%	76.78%
1e-2	89.03%	99.91%	86.50%	86.20%
1e-1	88.72%	99.98%	85.71%	94.92%

achieve good defense against adaptive attacks. However, the ASR of the model trained with NONE is still lower than that of the undefended model.